Pure & Appl. Chem., Vol. 69, No. 10, pp. 2105–2110, 1997.
Printed in Great Britain.

Ab initio molecular dynamics of rhodopsin

Angelo Bifone[a*], Huub J.M. de Groot[a] and Francesco Buda[b]

[a] *Leiden Institute of Chemistry, Leiden University, Gorlaeus Laboratories, P.O.Box 9502, 2300 RA Leiden, The Netherlands,*
[b] *INFM, Laboratorio Forum, Scuola Normale Superiore, I-56126, Pisa, Italy*

Abstract: We present a Car-Parrinello *ab initio* molecular dynamics study of the retinylidene chromophore of rhodopsin, the protein responsible for the first step in vision. The primary photochemical event involves an 11-*cis* to all-*trans* photo-isomerization of a protonated Schiff base of retinal. The ground-state structures of the two conformations of the chromophore, before and after the photon absorption, have been determined by a simulated annealing procedure. We compute the electrostatic and the torsional contributions to the energy storage in the primary photoproduct and study the role played by a counterion located in the vicinity of the chromophore. We also analyse localization and dynamics of a positively charged soliton on the chromophore backbone. The non-planarity of the chromophore results in a strong coupling of the soliton dynamics to the out-of-plane hydrogen oscillations, which may be relevant for the photoinduced isomerization process.

INTRODUCTION

The cascade of biochemical reactions that is responsible for light detection and signal transduction in the visual system is initiated by the photo-induced conformational change of a 7-helix protein, rhodopsin, in the membranes of the rod cells (ref. 1). This conformational change is triggered by the photo-isomerization of a Protonated Schiff Base of Retinal (RPSB) (Fig. 1), the chromophore of this and other important biological photoreceptors, *e.g.* bacteriorhodopsin, the proton-pumping protein of *Halobacterium halobium* (ref. 1). The 11-*cis* to all-*trans* isomerization of the retinylidene chromophore of rhodopsin upon absorption of a photon is completed within a very short time, 200 fs, and is one of the fastest photochemical reactions (ref. 2). This process is characterized by a high quantum yield of 65% and by high efficiency in energy conversion, as 33Kcal/mol (ref.1), ≈80% of the energy of the photon, are stored in the primary photoproduct, bathorhodopsin, an all-*trans* form of the retinylidene chromophore (ref. 1).

In this paper we present a study of the structural and dynamic properties of the chromophores of rhodopsin and bathorhodopsin within a Car-Parrinello *ab initio* molecular dynamics approach (ref. 3), based on the Density Functional Theory within the Local Density Approximation (DFT-LDA). This first

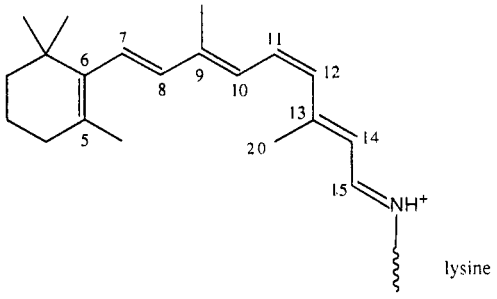

Fig. 1 Formula of the 11-*cis* retinal protonated Schiff base.

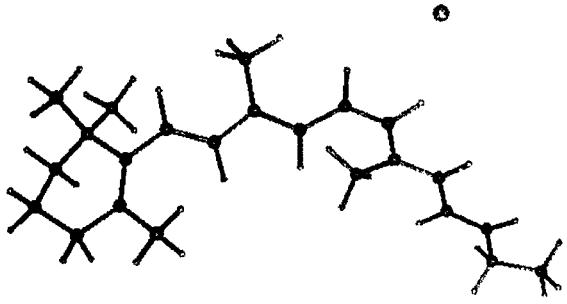

Fig.2 Optimized structure of the RPSB of rhodopsin, including the experimental constraints.

principles technique allows us to optimize fully the geometry of the molecule with a simulated annealing procedure, an efficient approach to overcome local minima in the Born-Oppenheimer hypersurface. Moreover, *ab initio* molecular dynamics makes it possible to study simultaneously the dynamic evolution of the atomic positions and of the electronic ground state. This is crucial to studying the dynamics of a conjugated system, where the electronic and vibrational degrees of freedom are effectively coupled. We show that the *cis-trans* isomerization of the chromophore leads to a highly strained all-*trans* form in bathorhodopsin, where the energy is mainly stored in torsional distortions of the conjugated backbone. This configuration is obtained from the structure of the RPSB of rhodopsin with relatively small atom displacements, compatible with the very short time of formation of the primary photoproduct. The role of the negatively charged counterion is discussed. The MD simulation shows that the RPSB supports a propagating conjugation defect, which may drive the photoisomerization. The propagating conjugation defect carries the charge along the conjugated backbone. This soliton-like coherent charge propagation is strongly coupled to the vibrational degrees of freedom, due to the nonplanarity of the chromophore.

COMPUTATIONAL METHODS

The *ab initio* molecular dynamics approach describes the Newtonian dynamics of a system by using an interatomic potential obtained at each time-step from the instantaneous electronic ground state (ref. 3). The electronic structure is obtained within the Density Functional Theory (DFT) in the Local Density Approximation (LDA) using the Perdew and Zunger (ref. 4) parametrization of numerical quantum Monte Carlo results. We have included Gradient Corrections (GC) to the exchange-correlation functional in the form proposed by Becke and Perdew (ref. 5). Density Functional Theory in Local Density Approximation (DFT-LDA) studies of infinite chains have shown severe limitations in the description of the dimerization (ref. 6). However, we have recently shown that the Car-Parrinello method provides an excellent framework to study retinals (ref. 7). In fact, in such short conjugated chains the bond alternation is determined by the asymmetry of the molecule, and is stabilized by the β-ring, the side-chain methyl groups and the highly electrophilic tail (ref. 7). Soft first-principles pseudopotentials (ref. 8) have been used to describe the interactions of the valence electrons with the inner cores. The Kohn-Sham single particle wavefunctions are expanded on a plane wave basis set with an energy cut-off of 20 Ry. We have tested the convergence of the calculation relative to the energy cut-off on a C_2H_6 and a HCN molecule up to 30 Ry. At 20 Ry the C-C and C-N bond lengths are already close to the fully converged values within 1.0 %. The C-C and the C-N stretch frequencies are accurate within 1.0 % and 2.0 %, respectively. The expansion in plane waves implies the use of periodic boundary conditions. We have used a simulation box of 36×22×22 au, large enough to avoid interaction with the images.

bond	rho	batho	RSB
C5=C6	1.370	1.376	1.370
C6–C7	1.460	1.445	1.460
C7=C8	1.367	1.380	1.367
C8–C9	1.442	1.425	1.442
C9=C10	1.388	1.402	1.388
C10–C11	1.422	1.402	1.422
C11=C12	1.389	1.400	1.389
C12–C13	1.423	1.407	1.445
C13=C14	1.406	1.420	1.378
C14–C15	1.391	1.383	1.453
C15=N	1.342	1.359	1.294

Tab. 1 Computed carbon-carbon bondlengths (in Å) for the optimized structures of: an 11-*cis* RPSB, including the counterion and the structural constraints (rho); bathorhodopsin, including the counterion (batho); unprotonated Schiff Base of Retinal (RSB).

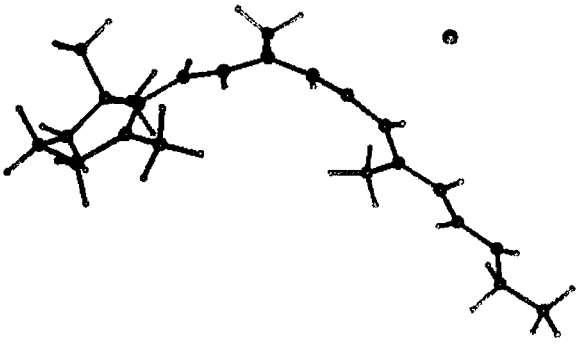

Fig.3 Optimized structure of the chromophore of bathorhodopsin. The chromophore presents a highly distorted all-*trans* configuration.

MODEL OF THE CHROMOPHORE OF RHODOPSIN

The geometric and electronic structures of the retinal chromophore in rhodopsin are sensitive to the interactions with the protein, which ultimately determine the function of the RPSB. The steric interaction of the methyl group bound to C13 with the protein induces a twist of the C12-C13 bond. This out-of-plane distortion of the chromophore affects the mechanism and the quantum efficiency of the isomerization process (ref. 9). We have modelled the chromophore with initial C20-C11 and C20-C10 distances of 3.0 Å and 3.05 Å, respectively, as determined by recent solid state NMR experiments (ref. 9). The chromophore has been terminated with a $-CH_2-CH_3$ group to mimic the linkage to the protein via lysine. The protonation of the retinal-lysine Schiff base adds a net positive charge to the chromophore. Two-photon absorption studies indicate a neutral binding site (ref. 1 and references therein), which implies a negatively charged counterion in the close vicinity of the chromophore. The electrostatic interaction between the retinal and the counterion contributes to locking the protein in an inactive state in the dark and to tuning the chromophore optical absorption. In our simulation, the counterion has been modelled by including a chlorine ion (Cl^-) placed at 4 Å from C12. Although much simpler than the actual counterion, a glutamate residue, this counterion captures the essential electrostatic interaction (ref. 10).

GROUND STATE STRUCTURE

The ground state equilibrium structures of the RPSB of rhodopsin (Fig. 2) and bathorhodopsin (Fig. 3) have been calculated with a simulated annealing procedure. The C20-C11 and C20-C10 distances in rhodopsin after the optimization procedure are 3.05 Å and 3.08 Å, respectively, and do not substantially differ from the initial values. The carbon-carbon bond lengths along the backbone chain are reported in Table 1. The rhodopsin RPSB presents clear bond alternation, except for the terminal region close to the nitrogen atom. For comparison, we have also reported the carbon-carbon distances for a neutral Schiff base, which presents bond alternation along the entire backbone. Thus, the protonation of the Schiff base introduces an extra positive charge in the chromophore, which induces a conjugation defect (ref. 11). This defect is localized adjacent to the electronegative nitrogen (Tab. 1). Optimization of the structure of the rhodopsin RPSB without a counterion yields qualitatively similar results, but the conjugation defect is more delocalized along the conjugated backbone. The dynamics of this charged defect or soliton will be described in the next section.

The structure of the bathorhodopsin RPSB has been optimized starting from the minimum energy rhodopsin RPSB structure, with the hydrogen bound to C12 displaced in a *trans* position with respect to the hydrogen bound to C11. The severe strain in this distorted all-*trans* structure induces a chain deformation, and leads to the equilibrium structure reported in Fig. 3. The time scale for this readjustment is of the order of 100 fs, and is compatible with the time of formation of the primary photoproduct. The bow-like structure of Fig. 3, in fact, is obtained with relatively small atomic displacements from the 11-*cis* configuration. Specifically, the angle between the two planes formed, for instance, by (C7,C8,C9) and (C13,C14,C15) changes from an initial value of about 40° to 110° in approximately 145 fs. The hinge of this motion is the bond C10-C11. C4, C5 and C6 are also involved in the readjustment, while the displacements of the other atoms of the ring are negligible.

The conjugation defect, which is induced by the excess positive charge on the backbone, is much broader in bathorhodopsin, and is located on C9 when the optimization is performed without the counterion. This is apparent from the inversion of bond alternation in the tail of the molecule. In fact, the displacement of the conjugation defect results in a bond order inversion, in the fashion of a charged soliton displacement in a conjugated chain (ref. 11). Thus, the bare retinylidene chromophore shows a bistable structure. This is incompatible with the NMR data (ref. 12), which show that no dramatic charge rearrangement occurs when the primary photoproduct is formed. The total energy in the bathorhodopsin model RPSB without the counterion is about 18 kcal/mol higher than in the rhodopsin RPSB. When the counterion is included in the model, the optimized structure of the bathorhodopsin RPSB presents the charged defect in the terminal region of the tail, in the same position as in rhodopsin, although more delocalized. Thus, the electrostatic interaction with the counterion locks the conjugation defect in the terminal region of the conjugated system and prevents charge displacement towards the ring, in agreement with the experiment (ref. 12).

The computed energy stored in this model bathorhodopsin RPSB including the counterion is 22 kcal/mol. The additional energy stored in the system is not related to the charge separation between chromophore and counterion, but rather to greater molecular stiffness. In fact, the interaction with the counterion increases the dimerization of the conjugated chain and prevents charge rearrangement along the backbone, which would decrease the π character of the double bonds and release part of the strain. Thus, a counterion is crucial to the energy storage in our model bathorhodopsin, since it affects the structural properties of the chromophore.

The steric hindrance of the methyl group bound to C13 induces an out-of-plane deformation of the chromophore of rhodopsin (Fig.4). In our model of the rhodopsin RPSB, the deformation is distributed along the backbone. The dihedral angles in the region C9-C14 of rhodopsin present significant deviations from planarity. The total out-of-plane deformation is approximately 40 degrees, but the individual bond twists are small. The bathorhodopsin RPSB presents a highly strained all-*trans* backbone (fig.3). Noticeably, while the deviations from planarity calculated for the C-C-C-C groups are large, the deviations for the H-C-C-H groups are much smaller. In fact, the distortion includes twists around the bonds as well as bends of the backbone, as apparent from the bow-like structure of Fig. 3. The out-of-plane displacements of the hydrogen atoms are distributed over the chain and are relatively small. This is consistent with the experimental observation that the hydrogen out-of-plane vibrational modes are similar in rhodopsin and bathorhodopsin (ref. 13).

The energy stored in our model of bathorhodopsin is lower than the experimental value. This may be due to an incomplete dimerization in the computed structure of the RPSB. In retinals, similar calculations yield a slightly underestimated dimerization amplitude (ref. 7). Moreover, the energy stored in the chromophore of bathorhodopsin depends considerably on fine details of the starting RPSB structure, and on the counterion structure and its distance from the chromophore. In addition, water molecules in the binding pocket and interactions with other protein residues may also play a role. Unfortunately, these details have not been experimentally characterized yet. Nevertheless, the mechanisms described above depend on the fundamental physical properties of the system, and are generally applicable.

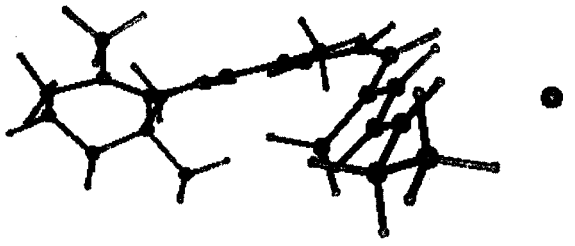

Fig. 4 The steric interactions with the binding pocket induce an out-of-plane deformation of the chromophore of rhodopsin.

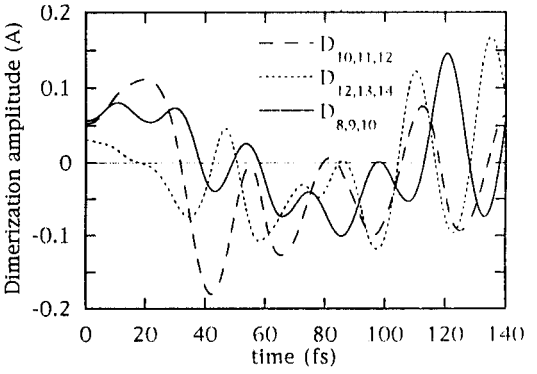

Fig.5 Dimerization amplitudes (defined as the difference between adjacent C-C bond lengths) as a function of time during the molecular dynamics simulation. $D_{i,j,k}=d_{i,j}-d_{j,k}$, where $d_{i,j}$ denotes the Ci-Cj bond length.

SOLITON DYNAMICS

In order to obtain the equilibrium structure of bathorhodopsin, we have isomerized the chromophore of rhodopsin brute force by flipping the hydrogen bound to C12 to a *trans* position with respect to the hydrogen of C11. When the system in such a highly distorted all-*trans* configuration is allowed to evolve in a microcanonical molecular dynamics simulation, the backbone readjusts to release the strain. The molecular dynamics has revealed an unexpected relaxation pathway. In fact, the potential energy stored in the retinal is transferred into kinetic energy of the atoms and a coherent propagation of the positively charged conjugation defect along the backbone is observed. This propagation induces an inversion of the single-double bond alternation, in the fashion of a positively charged soliton. This analogy makes it natural to compare the conjugation defect in RPSB to a soliton (ref. 14, 15), although the concept of soliton is rigorously defined only for an infinite conjugated chain. Figure 5 shows the time dependence of the dimerization amplitudes (defined as the difference between adjacent C-C bond lengths) at various positions along the backbone. An inversion of the bond order in this representation corresponds to a change of sign in the dimerization amplitudes. An inversion in the bond alternation for the C12-C13 and C13-C14 bonds occurs after about 20 fs, followed by an inversion for C10-C11 and C11-C12, and for C8-C9 and C9-C10, after 35 fs and 40 fs, respectively. This corresponds to a propagation of the positively charged conjugation defect towards the β-ring. The C6-C7 and C7-C8 bonds are also affected during the dynamics, but an inversion of bond order is never observed. When the defect reaches the β-ring, it is reflected back. Analogously, the defect is reflected at the Schiff base end, which prevents a propagation of the positive charge into the protein via the lysine group. Thus, the defect propagation is confined in the region C6-C15.

The charged defect propagates coherently along the planar part of the backbone with a velocity of 1.4 (±0.4)×10^6 cm/sec. When the soliton passes through the twisted region C9-C10-C11-C12, it couples strongly to out-of-plane oscillations of the molecule. This causes a transfer of energy into vibrational modes, with a consequent damping and loss of coherence of the defect propagation. The strong oscillations of the hydrogen atoms bound to C11 and C12 upon the passage of the defect support the model that a propagating coherent excitation may drive the isomerization of the chromophore.

Due to the low symmetry of the molecule, the vibrational spectra of retinals are dominated by highly localized vibrational modes (ref. 7). In the RPSB, however, an analysis of the atomic trajectories during the simulation reveals a low frequency collective vibrational feature at 270 cm^{-1}, which can be related to the

soliton propagation. This feature is apparent in all the longitudinal localized modes in the conjugated region, and is particularly evident in the Fourier transform of the time dependent dihedral angle C9-C10-C11-C12. Thus, the charge oscillation is associated with a collective slow mode, which arises from the coupling of the soliton propagation along the backbone to torsional modes of the chain. This coupling is determined by the non-planarity of the molecule. The incoherent energy transfer from the soliton to vibrational modes causes a damping of the coherent oscillation, as the system reaches thermal equilibrium. These results are consistent with Ultra Fast Optical Spectroscopy data (ref. 3), which show that the relaxation after photoisomerization is characterized by slow coherent oscillations that are rapidly damped after the primary photoproduct is formed. After 250 fs of simulation within microcanonical dynamics, we have cooled down the system with a simulated annealing procedure. The final equilibrium structure is the all-*trans* configuration of Fig.3.

CONCLUSION

In conclusion, we have studied the equilibrium structure and the dynamics of the chromophores of rhodopsin and of its primary photoproduct, bathorhodopsin, with a Car-Parrinello *ab initio* molecular dynamics approach. Bathorhodopsin presents a highly strained all-*trans* form, where the energy is mainly stored in torsional distortions of the back-bone. The distortion is distributed along the entire conjugated chain. The positive charge resulting from the protonation of the Schiff base induces a conjugation defect that is located in proximity of the terminal nitrogen. We have studied the dynamics of this defect, which propagates in the fashion of a positively charged soliton and is responsible for charge transport along the conjugated backbone. The dynamics of this soliton is strongly coupled to vibrational degrees of freedom, due to the non-planar structure of the molecule. The oscillation of the defect gives rise to a slow mode in the vibrational spectrum of the RPSB.

Acknowledgements We wish to thank Prof. J. Lugtenburg for his constant support and encouragement, and J. Shelley for the graphic package (MOVIE) used to visualize the results of the simulations. We are grateful to A. Curioni, J. Zaanen, F.L.J. Vos, D.P. Aalberts, W. van Saarloos for interesting discussions. The numerical calculations were performed in the Computer Centre of the Scuola Normale Superiore in Pisa, Italy. Research was partially supported by the EC Biotechnology program, contract CT930467. A.B. gratefully acknowledges financial support from SON-NWO.

* Present address: Institute of Cancer Research of the University of London, The Royal Marsden NHS Trust, Downs Road, Sutton, Surrey SM2 5PT, UK.

REFERENCES

1. R. R. Birge *Biochim. Biophys. Acta* **1016**, 293 (1990).
2. R. W. Schoenlein, L. A. Petenau, R. A. Mathies and C. V. Shank *Science* **254**, 412 (1991).
3. R. Car and M. Parrinello *Phys. Rev. Lett.* **55**, 2471 (1985).
4. J. P. Perdew and A. Zunger *Phys. Rev. B* **23**, 5048 (1981).
5. A. D. Becke *Phys. Rev. A* **38**, 3098 (1988).
6. J. Ashkenazi, W. E. Pickett, H. Krakauer, C. S. Wang, B. M. Klein and S. R. Chubb *Phys. Rev. Lett.* **62**, 2016 (1989).
7. A.Bifone, H.J.M. de Groot and F.Buda *Chem. Phys. Lett.* **248**, 165 (1996).
8. D. Vanderbilt *Phys. Rev. B* **43**, 7892 (1990).
9. P. Verdegem, P. Bovee-Geurts, W. de Grip, J. Lugtenburg and H.J.M. de Groot (manuscript in preparation).
10. M. Han , S. Decker and S. O. Smith *Biophys. J.* **65**, 899 (1993).
11. F. Buda, H.J.M. de Groot and A. Bifone (submitted).
12. S. O. Smith, J. Courtin, H. J. M. de Groot, R. Gebhard and J. Lugtenburg *Biochemistry* **30**, 7409 (1991).
13. I. Palings, J. A. Pardoen, E. van der Berg, J. Lugtenburg and R. A. Mathies *Biochemistry* **28**, 1498 (1989).
14. D. S. Chernavskii, Preprint 295, Moscow, FIAN (1986).
15. F. L. J. Vos, D. P. Aalberts and W. van Saarloos *Phys. Rev. B* **53**, 14922 (1996).